A functional genomics approach to understand host genetic regulation of COVID-19 severity

Yunus Kuijpers[1,2,+], Xiaojing Chu[1,2,3,+], Martin Jaeger[4], Simone J.C.F.M. Moorlag[4], Valerie A.C.M. Koeken[1,2,4], Vera P. Mourits[4], L. Charlotte J. de Bree[4], Quirijn de Mast[4], Frank L. van de Veerdonk[4], Leo A.B. Joosten[4,5], Yang Li[1,2,4], Mihai G. Netea[4,6,‡*], Cheng-Jian Xu[1,2,4,‡*]

[1]Centre for Individualised Infection Medicine, CiiM, a joint venture between the Hannover Medical School and the Helmholtz Centre for Infection Research, Hannover, Germany

[2]TWINCORE, Centre for Experimental and Clinical Infection Research, a joint venture between the Hannover Medical School and the Helmholtz Centre for Infection Research, Hannover, Germany

[3]Department of Genetics, University of Groningen, University Medical Center Groningen, Groningen, the Netherlands

[4]Department of Internal Medicine and Radboud Institute for Center for Infectious Diseases, Radboud University Medical Center, Nijmegen, the Netherlands

[5]Núcleo de Pesquisa da Faculdade da Polícia Militar (FPM) do Estado de Goiás, Goiânia, Goiás, Brasil

[6]Department for Genomics & Immunoregulation, Life and Medical Sciences Institute (LIMES), University of Bonn, Bonn, Germany

[†]shared first authors: these authors contribute equally.

[‡]shared senior authors: these authors contribute equally.

*Corresponding authors:

Mihai.Netea@radboudumc.nl; Xu.Chengjian@mh-hannover.de

One Sentence summary

In this study, we explore the physiological significance of the COVID-19 severity associated genetic variants using detailed clinical, immunological and multi-omics data from large cohorts. Our findings allow a physiological understanding of genetic susceptibility to severe COVID-19, and indicate pathways that could be targeted for prevention and therapy.

Abstract

A recent genome-wide association study of European ancestry has identified 3p21.31 and 9q34.2 (ABO gene) to be significantly associated with COVID-19 respiratory failure *(1)*. Here, we employed the detailed clinical, immunological and multi-omics data of the Human Functional Genomics Projects (HFGP) to explore the physiological significance of the host genetic variants that influence susceptibility to severe COVID-19. A functional genomics investigation based on functional characterization of individuals with high genetic risk for severe COVID-19 susceptibility identified several major patterns: i. a large impact of genetically determined innate immune responses in COVID-19, with increased susceptibility for severe disease in individuals with defective monocyte-derived cytokine production; ii. genetic susceptibility related to ABO blood groups is probably mediated through the von Willebrand factor (VWF) and endothelial dysfunction; and iii. the increased susceptibility for severe COVID-19 in men is at least partially mediated by chromosome X-mediated genetic variation. These insights allow a physiological understanding of genetic susceptibility to severe COVID-19, and indicate pathways that could be targeted for prevention and therapy.

Introduction

The novel coronavirus disease 2019 (COVID-19), caused by the severe acute respiratory syndrome coronavirus 2 (SARS-CoV-2) *(2)(3)*, firstly emerged in late December 2019 and has been spreading worldwide very quickly. The COVID-19 pandemic creates a severe disruption to the healthcare system and endangers the economy. As of the 21st of October, the World Health Organization has reported more than 40 million confirmed cases and over 1 million confirmed deaths *(4)*. While much has been learned about the pathophysiology of the disease, treatment proven to be effective is restricted to dexamethasone *(5)*, and there is no effective vaccine for COVID-19 yet. Therefore, there is an urgent need to better understand the exact host-pathogen interactions leading to increased severity and mortality, in order to design additional prophylactic and therapeutic strategies in future *(6)(7)*.

The severity of SARS-CoV-2 infection is highly variable, and ranges from asymptomatic to mild disease, and even to severe Acute Respiratory Distress Syndrome with a fatal outcome *(8)*. However, the causes for this broad variability in disease outcome between individuals are largely unknown. A recent study indicates that human host factors rather than viral genetic variation affect COVID-19 severity outcome *(9)*. Additionally, clinical and epidemiological data have shown that old age, male sex, and chronic comorbidity are associated with higher mortality *(10)(11)*. A recent genome-wide association study in individuals with genetic European ancestry has identified several chemokine receptor genes, including *CCR9*, *CXCR6* and *XCR1* and the locus controlling the ABO blood type to be associated with severe symptoms of COVID-19 *(1)*. Nevertheless, little is known about the mechanisms through which these genetic variants influence COVID-19 severity. For example, several competing hypotheses may be envisaged for the involvement of immune genes in susceptibility to severe COVID-19: on the one hand, it may be hypothesized that genetic risk for severe COVID-19 is associated

with defective innate immune responses that would allow viral multiplication with high viral loads; on the other hand, the opposite hypothesis may also be true, with an exaggerated genetically-mediated cytokine production being responsible for the late phase hyperinflammation and poor outcome. A purely genetic study cannot respond to this crucial question, that would have important consequences for the approach to prophylaxis and therapy.

By making use of resources from the Human Functional Genomics Project (HFGP) *(12, 13)*, we assessed the impact of COVID-19 associated genetic polymorphisms on variability of immune responses at the population level. This study will help us to understand how genetic variability is related to disease susceptibility through the regulation of immune responses and endothelial function.

Results

This study was conducted in two Dutch cohorts of healthy volunteers from HFGP: 451 participants from the 500 Functional Genomics (500FG) cohort *(12, 13)*, and 313 volunteers from the 300 Bacillus Calmette–Guérin (300BCG) cohort *(14)*. The basic characteristics of study populations are shown in Table S1.

COVID-19 loci are enriched for expression in immune organs, chemokine signaling pathways and enhancer region

To explore the functional impact of the identified COVID-19 loci, we firstly investigated if the identified independent genetic loci ($<1\times10^{-5}$) associated with severe COVID-19 are associated with any phenotypes available at the GWAS catalog (https://www.ebi.ac.uk/gwas/). We found that many of these loci are associated with immune traits such as blood protein, LDL and VLDL concentrations (Table S2). We next performed functional annotation of significant loci and

gene-mapping using FUMA*(15)*. The SNP2GENE function identified 32 independent SNPs located in 26 different loci which reached suggestive significance in this study (p-value $<1\times10^{-5}$, Table S3). Using multiple independent expression quantitative trait loci (eQTL) datasets, FUMA mapped 115 genes to these 26 genomic risk loci. Using RNA-seq data of 30 tissues from GTEx database (v8), we found significant enrichment of candidate genes in expression in immune organs such as spleen and blood (Fig.1A), suggesting that they are important tissues contributing to the pathophysiology of COVID-19 *(16)(17)*. Moreover, we observed the enrichment of candidate genes to be mainly expressed in small intestine and lung (Fig. 1A), suggesting that COVID-19 represents a multisystem illness with involvement of different organs, consistent with the respiratory and intestinal symptoms of the disease *(18)*.

Pathway analysis using these 115 genes showed a strong enrichment in chemokine binding and chemokine receptors binding (Fig. 1B), which is in line with the fact that chemokines can recruit immune cells to the site of infection and are critical for the function of the immune response *(19)*. In addition, chemokines have been reported as the most significantly elevated biomarkers in patients with severe COVID-19 on the intensive care unit *(17)*.

Considering that all SNPs in LD with the 32 independent loci (p-value $<1\times10^{-5}$) identified by the COVID-19 GWAS, were significantly enriched in the non-coding intronic region (p value = 0.036, Fisher's exact test) (Table S4), we next examined whether the COVID-19 associated variants are enriched in regulatory DNA elements. We interrogated all significant SNPs (p-value$<1\times10^{-5}$ and stricter thresholds) with histone marks and chromatin states of 24 blood cell-types in the Roadmap Epigenome Project *(20)*. We found that the COVID-19 genetic loci were strongly enriched for enhancer markers and weakly enriched in promoter marker (Table S5). The strong enrichment of COVID-19 loci in enhancer marks indicates that the associated

genetic variants are likely to be involved in the regulation of immunologically related functions. This finding also suggests that epigenetic mechanisms may play an important role in the pathogenesis of COVID-19 infection.

3p21.31 loci are associated with lower production of monocyte-derived cytokines

Severe COVID-19 is characterized by complex immune dysregulation, combining immune defective features with hyperinflammatory innate immune traits *(21)(22)*. However, these analyses in patients could be done only late during the disease, and whether genetic risk for severe COVID-19 is characterized by low or high innate immune responses in a non-infected person is not known. We therefore used the cytokine QTL data from the 500FG cohort *(13)* of the HFGP to test whether SNPs in 3p21.31 influence cytokine production upon stimulation. We checked all SNPs located within a 50 kilobase window of top variant rs11385942, and showed all nominal significant associations (p-value < 0.05, Fig. 2A). Interestingly, we observed that the risk alleles for a severe course of COVID-19 are consistently associated with lower production of monocyte-dependent cytokines (IL-6, IL-1β and TNF-α) upon various *in-vitro* stimulations (Fig. 2A). Of note, COVID-19 risk alleles also correspond to lower monocyte-derived cytokine production after influenza stimulation, a viral stimulus(Fig. 2A and B). It is thus tempting to speculate that the people who carry risk alleles may not respond properly to an initial virus infection, leading to high viral loads, subsequent systemic inflammation and poor outcome. Next, we tested whether the COVID-19 risk SNPs are associated with the levels of circulating cytokines in blood. Using the same cohort, we found that IL-18 and IL-18BP show a suggestive positive association with genetic risk of COVID-19 (Fig. S1).

Von Willebrand Factor (VWF) and lymphocytes are strongly colocalized with ABO loci

It is known that ABO blood group influences the plasma levels of von Willebrand factor (VWF)*(23)* and elevated VWF levels are associated with severe COVID-19 *(24)*. We therefore tested the association of ABO locus with VWF circulating concentrations from the individuals in the 500FG cohort. Of note, we found the risk allele rs687621-G is significantly associated with elevated levels of VWF (p-value = 9.58×10^{-20}) (Fig. 3A and B). Recent studies have reported that the VWF level is highly related to COVID-19 severity *(25, 26)*. As VWF level in plasma is an indicator of inflammation, endothelial activation and damage *(27)*, our results suggest that the association of VWF and COVID-19 severity is very likely mediated through genetic regulation.

We next tested if this specific locus is associated with immune functions. Interestingly, we observed consistent negative correlation of VWF and T-cell derived cytokine production in response to various *ex-vivo* stimulations (Fig. 3C and Fig. S2). In addition, the ABO locus led by the variant rs687621 also showed statistically significant co-localization with several immune-mediated traits, including cell counts of lymphocytes (Coloc analysis H4: 0.98), monocytes (Coloc analysis H4: 1), neutrophils (Coloc analysis H4: 0.8) and whole blood cells (Coloc analysis H4: 1) (Fig. 3D).

Men have a higher genetic severity risk of COVID-19 than women

Polygenic risk scores (PRS) combine multiple risk alleles and capture an individual's load of common genetic variants associated with a disease phenotype *(28)*. Using the summary statistics provided in the GWAS study *(1)*, we calculated the PRS for the samples from 500FG and 300BCG cohorts. Since higher mortality of COVID-19 has been reported to be associated with male sex and BMI *(10, 11)*, we investigated whether these host factors are associated with the PRS, a predictive measure of risk for development of severe COVID-19.

We firstly assessed if males have a higher genetic risk compared to females in 500FG. Hereby, we defined people with top 10% PRS as a high-risk group and those with bottom 10% PRS as a low-risk group. As shown in Fig. 4A, male tend to have higher severe COVID-19 risk than female (odd ratio: 1.47, 95% CI: 0.98-2.22, p-value = 0.045 (Fisher's exact test)) (Table S6). We next used different percentile cut-offs (15%, 20%, 25% and 30%) to re-define low and high-risk groups. Interestingly, we observed a consistent pattern that males have higher genetic risk (PRS) than females at different percentile cut-offs. These results can be replicated in a similar, but independent, cohort (300BCG, Fig. 4B). Meanwhile, the genetic risk difference between male and female can be attenuated when a loose cut-off has been defined. The meta-analysis of two cohorts showed a significant p-value at various percentile cut-offs (10%, 15%, 20%, 25%) and marginal significant p-value of 0.051 at the percentile cut-off of 30%. Furthermore, this result persisted when PRS was computed using summary statistics from the GWAS model after age and sex correction, reported in the original GWAS study (Table S7). When computing PRS while excluding variants from the X and Y chromosomes, the enrichment of men in the higher PRS group was less pronounced at most thresholds (Fig. 4C and D). This suggested that higher genetic severity risk at least partially originates from the SNPs in the sex chromosomes.

As obesity or overweight has been reported as a risk factor for serious illness or death from COVID-19, we tested if the PRS is associated with BMI (Fig. S3). We did not observe any significant correlation between PRS and BMI.

Discussion

Understanding the pathophysiology of COVID-19 is urgently needed for designing novel preventive and therapeutic approaches against the disease. One important tool for identifying the most important mechanisms mediating a disease is genomics: genetic variants that influence susceptibility or severity to a disease are usually located in genetic loci that impact important mechanisms for that particular disease. Using the information of a recently published GWAS assessing the severity of COVID-19 *(1)*, and the rich datasets available in the HFGP, we interrogated the mechanisms through which genetic variants associated with severe COVID-19 exert their effects.

Among the genetic loci associated with severe COVID-19, the 3p21.31 gene cluster has been well replicated by independent studies from the COVID-19 Host Genetics Initiative (https://www.covid19hg.org), and it was reported to be inherited by Neanderthals *(29)*. This locus is currently regarded as a marker of COVID-19 severity, but crucial information is missing: are the risk alleles in this locus (that encode several cytokines and chemokines) associated with a lower or higher cytokine production. The answer to this question is crucial for understanding COVID-19: a genetic risk associated with low cytokine production would imply that severe COVID-19 is the consequence of a relative immunodeficiency, while a high cytokine production associated with genetic risk would mean that severe COVID-19 is a genetic hyperinflammatory disease. In our study, the 3p21.31 genetic polymorphisms associated with a high risk of severe COVID-19 were associated with lower production of monocyte-derived cytokines, especially to viral (influenza) stimuli. This important discovery has significant prophylactic and therapeutic consequences. On the one hand, it implies that improvement of innate immune responses in healthy individuals would decrease the probability that they undergo a severe form of COVID-19: this supports the rationale of clinical trials that improve innate immune responses through induction of trained immunity, e.g. by vaccination

with BCG *(6)*. On the other hand, this also implies that the dysregulated immune responses that have been described at late time points in patients with severe COVID-19 *(30)(31)* are likely the consequence of accelerated viral multiplication due to defective innate immune responses, and subsequent systemic inflammation due to high viral loads.

Several studies have shown that ABO blood types are associated with COVID-19 severity *(32)(33)* and susceptibility *(34)(35)(36)*. It is still not well-known how ABO gene regulates COVID-19 susceptibility. As ABO blood group are also expressed on endothelial cells and platelets, it has been speculated that this effect may manifest itself via elevated plasma VWF *(37)*. Our results provide evidence supporting this hypothesis, by showing that the risk alleles in the ABO locus are associated with high concentrations of VWF. Moreover, interesting associations have been found between polymorphisms in this locus and the number of various immune cell populations, especially lymphocytes, since lymphopenia is also consistently associated with severe COVID-19 *(38)*. This suggests that genetic factors are relevant to the host thrombo-inflammatory response. However, a note of caution should be mentioned , as the association between the genetics of ABO group with severity in COVID-19 Host Genetics Initiative data did not reach a genome-wide level of significance (p value $<5\times10^{-8}$) (Table S8) (as of 21st of October 2020, and thus the association might be population specific.

Another important observation is that an important component of the impact of genetic polymorphisms on the severity of COVID-19 is mediated through sex chromosomes, most likely chromosome X which is known to encode many genes related to the immune system. Indeed, men in both 500FG and 300BCG cohorts had a higher genetic risk then women, and this difference was largely lost when sex chromosomes were excluded from the analysis. These data strongly argue that at least part of the well-known increase of COVID-19 severity in men

is genetically determined. The recent description by our group of rare mutations in the RNA receptor TLR7 located on chromosome X as a cause of very severe COVID-19 in young men supports this hypothesis *(39)*.

While our study sheds further light on how COVID-19 genetic risk affects the human immune system, there are several limitations of this study: firstly, due to different sets of stimuli used in measuring cytokine production to stimulations in the two healthy cohorts, we are not able to replicate all our findings of genetic associations with cytokine responses from the 500FG cohort in the 300BCG cohort. Secondly, young adults (< 30 years) are overrepresented in both healthy cohorts (500FG and 300BCG), which may lead to a biased conclusion which cannot be generalized to the whole population, especially since the severe COVID-19 cases often occur in the elderly population. Thirdly, 500FG and 300BCG cohorts are designed to understand the genetic regulation of immune function in healthy individuals. Therefore, a COVID-19 patients' cohort will be needed for better characterization of disease mechanism, which will be our future research goal.

Collectively, our data demonstrate that genetic variability explains an important component of the increased susceptibility to severe COVID-19. The genetic risk for severe COVID-19 is associated with defective innate immune responses (low cytokine production), dysregulated endothelial function, and is strongly influenced by polymorphisms in sex chromosomes. These findings may contribute to the development of novel treatment and prevention strategies for severe COVID-19.

Materials and Methods

Study cohort

The cohorts involved in this study are from the Human Functional Genomics Project (HFGP)*(40)*. 500FG consists of 451 healthy individuals of European ancestry with genotype measurement. Within this cohort, immune cell counts, cytokine production upon stimulations, platelets, globulins, and gut microbiome were measured (for detailed information see *(12, 13, 41, 42)*). 300BCG consists of 313 healthy Europeans that participated in a BCG vaccination study *(14)(43)*. Within this cohort, blood was collected before vaccination and cytokine production was measured upon *ex-vivo* stimulation of PBMCs with microbial stimuli.

Genotype quality control and imputation

Genotyping on samples from 500FG and 300BCG was performed using Illumina humanOmniExpress Exome-8 v1.0 SNP chip Calling by Opticall 0.7.0*(44)* with default settings. All individuals of non-European ancestry, ambiguous sex, call rate ≤ 0.99, excess of autosomal heterozygosity (F<mean-3SD), cryptic relatedness ($\pi>0.185$) were removed. SNPs with low genotyping rate (<95%), with low minor allele frequency (<0.001), deviation from Hardy-Weinberg equilibrium ($p<10^{-4}$) were excluded. The detailed QC steps have been published in reference(13). Genotype data of 500FG and 300BCG were imputed respectively. The imputation was performed on the Michigan imputation server*(45)*. The cohorts were phased using Eagle v2.4 with the European population of HRC 1.1 2016 hg 2019 reference panel. After imputation, variants with a MAF < 0.01, an imputation quality score R2 < 0.5, or a Hardy-Weinberg-Equilibrium $P < 10^{-12}$ were excluded. All quality control steps were performed using Plink v1.9. After imputation and quality control, 451 individuals from 500FG and 313 individuals from 300BCG were available for downstream analyses.

Immune parameter quantitative trait locus (QTL) profiles

We acquired summary statistics of cytokine QTLs *(13)*, cell proportion QTLs*(41)* and circulating metabolite QTLs*(46)* from our previous studies performed with 500FG. We performed QTL mapping for circulating mediators and platelet traits in 500FG using an R package MatrixeQTL*(47)*. The measurement of circulating mediators including IL-18BP, resistin, leptin, adiponectin, alpha-1 antitrypsin (AAT), and IL-18 have been described previously*(12)*. Platelet traits*(48)* include Thrombin-Antithrombin Complex (TAT), Beta-thromboglobulin total, beta-thromboglobulin, fibrinogen binding, collagen-related peptide (CRP) P-selectin, CRP fibrinogen, ADP P-selectin, ADP fibrinogen, P-selectin, platelet–monocyte complex, total platelet count, and von Willebrand factor (VWF). The circulating mediator levels and platelet traits were log2 transformed. A linear model was applied to the platelet data and genetic data by taking age and sex as covariates. We considered p-value $< 5\times10^{-8}$ to be genome-wide significant.

Colocalization analysis.

We performed co-localization analysis *(49)* to look at the overlapping profile between molecular QTLs, COVID-19 GWAS, and other GWAS profiles using the R package 'coloc'.

PRS calculation

Polygenic risk scores (PRS) were calculated by first intersecting the variants from the COVID-19 summary statistics*(1)* with the variants present in our samples. Clumping was done starting at the most significant variant. All variants within a 250kb window around that variant were excluded if they were in greater LD than 0.1 before continuing to the most significant variant outside of the previous window. For each sample specifically, we then multiplied the dosage of the effect allele with its effect size while substituting missing genotype data with the average

dosage of that variant in the entire sample set. These values were then summed to form the PRS for each specific sample. As the GWAS summary statistics for creating PRS from Eillinghaus *et.al (1)* did not correct age and sex, we also performed a sensitivity analysis with the PRS created from the GWAS model corrected for age and sex.

PRS based correlations

Linear models were constructed using the computed PRS and various phenotype data available for each cohort. Samples within the top/bottom 10% PRS were classified as high/low-risk, respectively. Using the PRS of the samples in these risk groups, we performed a Student T-test to test for significant correlation between gender and PRS. Furthermore, we tested for enrichment of any specific gender in these risk groups using a Fisher's exact test.

Functional analysis of genomic loci

We used the FUMA pipeline in order to identify genes linked to COVID-19 with severe respiratory failure. FUMA identified significant independent SNPs as variants with $P < 1\times10^{-5}$ that were independent from each other using an LD threshold of $r2 < 0.6$. Within these independent significant SNPs variants lead SNPs are identified as the most significant variants that are independent using an LD threshold of $r2 < 0.1$. We mapped Genes to these SNPs based on their genomic position allowing for a maximum distance of 10kb. In addition to this, genes were also mapped based on eQTL effects. Genes were selected based on significant SNP-gene pairs at FDR < 0.05 using cis- and trans-eQTLs from eQTLGen.

As part of the FUMA pipeline we used these mapped genes in order to generate gene expression heatmaps using GTEx v8 (54 tissue types and 30 general tissue types). Gene expression values with a pseudocount of 1 were normalized across tissue types using winsorization at 50 and log2

transformed. Using the hypergeometric test, we tested for significant enrichment of our input genes in DEG sets for the different tissue types using a Bonferroni corrected P value ≤ 0.05. Finally, we tested for overrepresentation of our input genes in predetermined gene-sets using hypergeometric tests. Gene-sets were obtained from MsigDB, WikiPathways, and GWAS-catalog reported gene-sets. We used Benjamini-Hochberg FDR correction for each of the categories within these gene-set sources separately using a threshold of 0.05 for our adjusted P value.

Roadmap epigenetic state enrichment

Based on the Roadmap 15-core epigenetic state database*(20)*, we used data obtained from 23 blood samples spanning 127 epigenomes to map the QTLs in the summary statistics to their respective epigenetic states. Epigenetic state information was available for bins of 200bp. we aggregated this information into 4 categories; active enhancer states (Enh, EnhG), active promotor states (TssA, TssAFlnk), all enhancer states (Enh, EnhG, EnhBiv), and all promotor states (TssA, TssAFlnk, TssBiv). We tested for enrichment using a Fisher's exact test based on the number of unique 200bp bins variants mapped to. This was done after filtering the QTL's down based on their p value using different thresholds (1×10^{-5}, 1×10^{-6} and 1×10^{-7}). Enrichment P values were obtained after FDR correction.

Visualization.

R package ggplot2 was used to perform bar charts, box plots and scatter plots. We applied an online tool Locus zoom to present genes within candidate loci. We used R package pheatmap to generate heat maps.

Acknowledgments:

We thank all volunteers in the 500FG and 300BCG cohorts of the Human Functional Genomics Project (HFGP) for their participation.

Funding

MGN was supported by an ERC Advanced Grant (833247) and a Spinoza Grant of the Netherlands Organization for Scientific Research. YL was supported by an ERC starting Grant (948207) and a Radboud University Medical Centre Hypatia Grant (2018). CJX was supported by Helmholtz Initiative and Networking Fund (1800167).

Author contributions

M.G.N., C.J.X. and Y.L. designed the study, Y.K. and X.C. performed statistical analyses supervised by Y.L. and C.J.X., M.J., S.M., V.K., V.M., C.d.B., Q.d.M. and L.A.B.J. established the cohorts, helped with the data analysis and interpretation of results. C.J.X., M.G.N., Y.L., Y.K. and X.C. wrote the manuscript with input from all authors.

Competing interests

The authors declare no competing interests.

Data and materials availability:

500FG data used in this project have been archived in the BBMRI-NL data infrastructure (https://hfgp.bbmri.nl/). This allows flexible data querying and download, including sufficiently rich metadata and interfaces for machine processing and using FAIR principles to optimize Findability, Accessibility, Interoperability and Reusability.

Ethics statement

The 300BCG (NL58553.091.16) and 500FG (NL42561.091.12) studies were approved by the Arnhem-Nijmegen Medical Ethical Committee. Experiments were conducted according to the principles expressed in the Declaration of Helsinki. Samples of venous blood were drawn after informed consent was obtained.

References

1. D. Ellinghaus, F. Degenhardt, L. Bujanda, M. Buti, A. Albillos, P. Invernizzi, J. Fernández, D. Prati, G. Baselli, R. Asselta, M. M. Grimsrud, C. Milani, F. Aziz, J. Kässens, S. May, M. Wendorff, L. Wienbrandt, F. Uellendahl-Werth, T. Zheng, X. Yi, R. de Pablo, A. G. Chercoles, A. Palom, A.-E. Garcia-Fernandez, F. Rodriguez-Frias, A. Zanella, A. Bandera, A. Protti, A. Aghemo, A. Lleo, A. Biondi, A. Caballero-Garralda, A. Gori, A. Tanck, A. Carreras Nolla, A. Latiano, A. L. Fracanzani, A. Peschuck, A. Julià, A. Pesenti, A. Voza, D. Jiménez, B. Mateos, B. Nafria Jimenez, C. Quereda, C. Paccapelo, C. Gassner, C. Angelini, C. Cea, A. Solier, D. Pestaña, E. Muñiz-Diaz, E. Sandoval, E. M. Paraboschi, E. Navas, F. García Sánchez, F. Ceriotti, F. Martinelli-Boneschi, F. Peyvandi, F. Blasi, L. Téllez, A. Blanco-Grau, G. Hemmrich-Stanisak, G. Grasselli, G. Costantino, G. Cardamone, G. Foti, S. Aneli, H. Kurihara, H. ElAbd, I. My, I. Galván-Femenia, J. Martín, J. Erdmann, J. Ferrusquía-Acosta, K. Garcia-Etxebarria, L. Izquierdo-Sanchez, L. R. Bettini, L. Sumoy, L. Terranova, L. Moreira, L. Santoro, L. Scudeller, F. Mesonero, L. Roade, M. C. Rühlemann, M. Schaefer, M. Carrabba, M. Riveiro-Barciela, M. E. Figuera Basso, M. G. Valsecchi, M. Hernandez-Tejero, M. Acosta-Herrera, M. D'Angiò, M. Baldini, M. Cazzaniga, M. Schulzky, M. Cecconi, M. Wittig, M. Ciccarelli, M. Rodríguez-Gandía, M. Bocciolone, M. Miozzo, N. Montano, N. Braun, N. Sacchi, N. Martínez, O. Özer, O. Palmieri, P. Faverio, P. Preatoni, P. Bonfanti, P. Omodei, P. Tentorio, P. Castro, P. M. Rodrigues, A. Blandino Ortiz, R. de Cid, R. Ferrer, R. Gualtierotti, R. Nieto, S. Goerg, S. Badalamenti, S. Marsal, G. Matullo, S. Pelusi, S. Juzenas, S. Aliberti, V. Monzani, V. Moreno, T. Wesse, T. L. Lenz, T. Pumarola, V. Rimoldi, S. Bosari, W. Albrecht, W. Peter, M. Romero-Gómez, M. D'Amato, S. Duga, J. M. Banales, J. R. Hov, T. Folseraas, L. Valenti, A. Franke, T. H. Karlsen, Genomewide Association Study of Severe Covid-19 with Respiratory Failure, *N Engl J Med* (2020), doi:10.1056/NEJMoa2020283.

2. F. Wu, S. Zhao, B. Yu, Y.-M. Chen, W. Wang, Z.-G. Song, Y. Hu, Z.-W. Tao, J.-H. Tian, Y.-Y. Pei, M.-L. Yuan, Y.-L. Zhang, F.-H. Dai, Y. Liu, Q.-M. Wang, J.-J. Zheng, L. Xu, E. C. Holmes, Y.-Z. Zhang, A new coronavirus associated with human respiratory disease in China, *Nature* **579**, 265–269 (2020).

3. P. Zhou, X.-L. Yang, X.-G. Wang, B. Hu, L. Zhang, W. Zhang, H.-R. Si, Y. Zhu, B. Li, C.-L. Huang, H.-D. Chen, J. Chen, Y. Luo, H. Guo, R.-D. Jiang, M.-Q. Liu, Y. Chen, X.-R. Shen, X. Wang, X.-S. Zheng, K. Zhao, Q.-J. Chen, F. Deng, L.-L. Liu, B. Yan, F.-X. Zhan, Y.-Y. Wang, G.-F. Xiao, Z.-L. Shi, A pneumonia outbreak associated with a new coronavirus of probable bat origin, *Nature* **579**, 270–273 (2020).

4. World Health Organization, WHO Coronavirus Disease (COVID-19) Dashboard, https://covid19.who.int/ (2020) (available at https://covid19.who.int/).

5. RECOVERY Collaborative Group, P. Horby, W. S. Lim, J. R. Emberson, M. Mafham, J. L. Bell, L. Linsell, N. Staplin, C. Brightling, A. Ustianowski, E. Elmahi, B. Prudon, C. Green, T. Felton, D. Chadwick, K. Rege, C. Fegan, L. C. Chappell, S. N. Faust, T. Jaki, K. Jeffery, A. Montgomery, K. Rowan, E. Juszczak, J. K. Baillie, R. Haynes, M. J. Landray, Dexamethasone in Hospitalized Patients with Covid-19 - Preliminary Report, *N Engl J Med* (2020), doi:10.1056/NEJMoa2021436.

6. M. G. Netea, E. J. Giamarellos-Bourboulis, J. Domínguez-Andrés, N. Curtis, R. van Crevel, F. L. van de Veerdonk, M. Bonten, Trained Immunity: a Tool for Reducing Susceptibility to and the Severity of SARS-CoV-2 Infection, *Cell* **181**, 969–977 (2020).

7. M. Z. Tay, C. M. Poh, L. Rénia, P. A. MacAry, L. F. P. Ng, The trinity of COVID-19: immunity, inflammation and intervention, *Nature Reviews Immunology* **20**, 363–374 (2020).

8. R. Verity, L. C. Okell, I. Dorigatti, P. Winskill, C. Whittaker, N. Imai, G. Cuomo-Dannenburg, H. Thompson, P. G. T. Walker, H. Fu, A. Dighe, J. T. Griffin, M. Baguelin, S. Bhatia, A. Boonyasiri, A. Cori, Z. Cucunubá, R. FitzJohn, K. Gaythorpe, W. Green, A. Hamlet, W. Hinsley, D. Laydon, G. Nedjati-Gilani, S. Riley, S. van Elsland, E. Volz, H. Wang, Y. Wang, X. Xi, C. A. Donnelly, A. C. Ghani, N. M. Ferguson, Estimates of the severity of coronavirus disease 2019: a model-based analysis, *The Lancet Infectious Diseases* **20**, 669–677 (2020).

9. X. Zhang, Y. Tan, Y. Ling, G. Lu, F. Liu, Z. Yi, X. Jia, M. Wu, B. Shi, S. Xu, J. Chen, W. Wang, B. Chen, L. Jiang, S. Yu, J. Lu, J. Wang, M. Xu, Z. Yuan, Q. Zhang, X. Zhang, G. Zhao, S. Wang, S. Chen, H. Lu, Viral and host factors related to the clinical outcome of COVID-19, *Nature* **583**, 437–440 (2020).

10. G. Chen, D. Wu, W. Guo, Y. Cao, D. Huang, H. Wang, T. Wang, X. Zhang, H. Chen, H. Yu, X. Zhang, M. Zhang, S. Wu, J. Song, T. Chen, M. Han, S. Li, X. Luo, J. Zhao, Q. Ning, Clinical and immunological features of severe and moderate coronavirus disease 2019, *Journal of Clinical Investigation* **130**, 2620–2629 (2020).

11. A. B. Docherty, E. M. Harrison, C. A. Green, H. E. Hardwick, R. Pius, L. Norman, K. A. Holden, J. M. Read, F. Dondelinger, G. Carson, L. Merson, J. Lee, D. Plotkin, L. Sigfrid, S. Halpin, C. Jackson, C. Gamble, P. W. Horby, J. S. Nguyen-Van-Tam, A. Ho, C. D. Russell, J. Dunning, P. J. Openshaw, J. K. Baillie, M. G. Semple, Features of 20 133 UK patients in hospital with covid-19 using the ISARIC WHO Clinical Characterisation Protocol: prospective observational cohort study, *BMJ* **369**, m1985 (2020).

12. R. ter Horst, M. Jaeger, S. P. Smeekens, M. Oosting, M. A. Swertz, Y. Li, V. Kumar, D. A. Diavatopoulos, A. F. M. Jansen, H. Lemmers, H. Toenhake-Dijkstra, A. E. van Herwaarden, M. Janssen, R. G. van der Molen, I. Joosten, F. C. G. J. Sweep, J. W. Smit, R. T. Netea-Maier, M. M. J. F. Koenders, R. J. Xavier, J. W. M. van der Meer, C. A. Dinarello, N. Pavelka, C. Wijmenga, R. A. Notebaart, L. A. B. Joosten, M. G. Netea, Host and Environmental Factors Influencing Individual Human Cytokine Responses, *Cell* **167**, 1111-1124.e13 (2016).

13. Y. Li, M. Oosting, S. P. Smeekens, M. Jaeger, R. Aguirre-Gamboa, K. T. T. Le, P. Deelen, I. Ricaño-Ponce, T. Schoffelen, A. F. M. Jansen, M. A. Swertz, S. Withoff, E. van de Vosse, M. van Deuren, F. van de Veerdonk, A. Zhernakova, J. W. M. van der Meer, R. J. Xavier, L. Franke, L. A. B. Joosten, C. Wijmenga, V. Kumar, M. G. Netea, A Functional Genomics Approach to Understand Variation in Cytokine Production in Humans, *Cell* **167**, 1099-1110.e14 (2016).

14. V. A. C. M. Koeken, L. C. J. de Bree, V. P. Mourits, S. J. C. F. M. Moorlag, J. Walk, B. Cirovic, R. J. W. Arts, M. Jaeger, H. Dijkstra, H. Lemmers, L. A. B. Joosten, C. S. Benn, R. van Crevel, M. Netea, BCG vaccination in humans inhibits systemic inflammation in a sex-dependent manner, *J Clin Invest* (2020), doi:10.1172/JCI133935.

15. K. Watanabe, E. Taskesen, A. van Bochoven, D. Posthuma, Functional mapping and annotation of genetic associations with FUMA, *Nature Communications* **8**, 1826 (2017).

16. X. Xu, X. Chang, H. Pan, H. Su, B. Huang, M. Yang, D. Luo, M. Weng, L. Ma, X. Nie, [Pathological changes of the spleen in ten patients with coronavirus disease 2019(COVID-19) by postmortem needle autopsy], *Zhonghua bing li xue za zhi = Chinese journal of pathology* **49**, 576–582 (2020).

17. F. L. van de Veerdonk, N. A. F. Janssen, I. Grondman, A. H. de Nooijer, V. A. C. M. Koeken, V. Matzaraki, C. K. Boahen, V. Kumar, M. Kox, H. J. P. M. Koenen, R. L. Smeets, I. Joosten, R. J. M. Br&uumlggemann, I. J. E. Kouijzer, H. G. van der Hoeven, J. A. Schouten, T. Frenzel, M. Reijers, W. Hoefsloot, A. S. M. Dofferhoff, A. P. M. Kerckhoffs, M. J. T. Blaauw, K. Veerman, C. Maas, A. H. Schoneveld, I. E. Hoefer, L. P. G. Derde, L. Willems, E. Toonen, M. van Deuren, J. W. M. van der Meer, R. van Crevel, E. J. Giamarellos-Bourboulis, L. A. B. Joosten, M. M. van den Heuvel, J. Hoogerwerf, Q. de Mast, P. Pickkers, M. G. Netea, A systems approach to inflammation identifies therapeutic targets in SARS-CoV-2 infection, *medRxiv* , 2020.05.23.20110916 (2020).

18. C. Robba, D. Battaglini, P. Pelosi, P. R. M. Rocco, Multiple organ dysfunction in SARS-CoV-2: MODS-CoV-2, *Expert Review of Respiratory Medicine* , 1–4 (2020).

19. C. Esche, C. Stellato, L. A. Beck, Chemokines: Key Players in Innate and Adaptive Immunity, *Journal of Investigative Dermatology* **125**, 615–628 (2005).

20. Roadmap Epigenomics Consortium, A. Kundaje, W. Meuleman, J. Ernst, M. Bilenky, A. Yen, A. Heravi-Moussavi, P. Kheradpour, Z. Zhang, J. Wang, M. J. Ziller, V. Amin, J. W. Whitaker, M. D. Schultz, L. D. Ward, A. Sarkar, G. Quon, R. S. Sandstrom, M. L. Eaton, Y.-C. Wu, A. R. Pfenning, X. Wang, M. Claussnitzer, Y. Liu, C. Coarfa, R. A. Harris, N. Shoresh, C. B. Epstein, E. Gjoneska, D. Leung, W. Xie, R. D. Hawkins, R. Lister, C. Hong, P. Gascard, A. J. Mungall, R. Moore, E. Chuah, A. Tam, T. K. Canfield, R. S. Hansen, R. Kaul, P. J. Sabo, M. S. Bansal, A. Carles, J. R. Dixon, K.-H. Farh, S. Feizi, R. Karlic, A.-R. Kim, A. Kulkarni, D. Li, R. Lowdon, G. Elliott, T. R. Mercer, S. J. Neph, V. Onuchic, P. Polak, N. Rajagopal, P. Ray, R. C. Sallari, K. T. Siebenthall, N. A. Sinnott-Armstrong, M. Stevens, R. E. Thurman, J. Wu, B. Zhang, X. Zhou, A. E. Beaudet, L. A. Boyer, P. L. De Jager, P. J. Farnham, S. J. Fisher, D. Haussler, S. J. M. Jones, W. Li, M. A. Marra, M. T. McManus, S. Sunyaev, J. A. Thomson, T. D. Tlsty, L.-H. Tsai, W. Wang, R. A. Waterland, M. Q. Zhang, L. H. Chadwick, B. E. Bernstein, J. F. Costello, J. R. Ecker, M. Hirst, A. Meissner, A. Milosavljevic, B. Ren, J. A. Stamatoyannopoulos, T. Wang, M. Kellis, Integrative analysis of 111 reference human epigenomes, *Nature* **518**, 317–330 (2015).

21. E. J. Giamarellos-Bourboulis, M. G. Netea, N. Rovina, K. Akinosoglou, A. Antoniadou, N. Antonakos, G. Damoraki, T. Gkavogianni, M.-E. Adami, P. Katsaounou, M. Ntaganou, M. Kyriakopoulou, G. Dimopoulos, I. Koutsodimitropoulos, D. Velissaris, P. Koufargyris, A. Karageorgos, K. Katrini, V. Lekakis, M. Lupse, A. Kotsaki, G. Renieris, D. Theodoulou, V. Panou, E. Koukaki, N. Koulouris, C. Gogos, A. Koutsoukou, Complex Immune Dysregulation in COVID-19 Patients with Severe Respiratory Failure, *Cell Host & Microbe* **27**, 992-1000.e3 (2020).

22. P. Mehta, D. F. McAuley, M. Brown, E. Sanchez, R. S. Tattersall, J. J. Manson, COVID-19: consider cytokine storm syndromes and immunosuppression, *The Lancet* **395**, 1033–1034 (2020).

23. M. Franchini, F. Capra, G. Targher, M. Montagnana, G. Lippi, Relationship between ABO blood group and von Willebrand factor levels: from biology to clinical implications, *Thrombosis Journal* **5**, 14 (2007).

24. G. Goshua, A. B. Pine, M. L. Meizlish, C.-H. Chang, H. Zhang, P. Bahel, A. Baluha, N. Bar, R. D. Bona, A. J. Burns, C. S. Dela Cruz, A. Dumont, S. Halene, J. Hwa, J. Koff, H. Menninger, N. Neparidze, C. Price, J. M. Siner, C. Tormey, H. M. Rinder, H. J. Chun, A. I. Lee, Endotheliopathy in COVID-19-associated coagulopathy: evidence from a single-centre, cross-sectional study, *The Lancet Haematology* **7**, e575–e582 (2020).

25. Aksenova A.Y., Von Willebrand factor and endothelial damage: a possible association with COVID-19, *EcoGen* **18**, 135–138 (2020).

26. A. V. Rapkiewicz, X. Mai, S. E. Carsons, S. Pittaluga, D. E. Kleiner, J. S. Berger, S. Thomas, N. M. Adler, D. M. Charytan, B. Gasmi, J. S. Hochman, H. R. Reynolds, Megakaryocytes and platelet-fibrin thrombi characterize multi-organ thrombosis at autopsy in COVID-19: A case series, *EClinicalMedicine* **24** (2020), doi:10.1016/j.eclinm.2020.100434.

27. C. Kawecki, P. J. Lenting, C. V. Denis, von Willebrand factor and inflammation, *Journal of Thrombosis and Haemostasis* **15**, 1285–1294 (2017).

28. A. V. Khera, M. Chaffin, K. G. Aragam, M. E. Haas, C. Roselli, S. H. Choi, P. Natarajan, E. S. Lander, S. A. Lubitz, P. T. Ellinor, S. Kathiresan, Genome-wide polygenic scores for common diseases identify individuals with risk equivalent to monogenic mutations, *Nature Genetics* **50**, 1219–1224 (2018).

29. H. Zeberg, S. Pääbo, The major genetic risk factor for severe COVID-19 is inherited from Neanderthals, *Nature* (2020), doi:10.1038/s41586-020-2818-3.

30. J. Schulte-Schrepping, N. Reusch, D. Paclik, K. Baßler, S. Schlickeiser, B. Zhang, B. Krämer, T. Krammer, S. Brumhard, L. Bonaguro, E. De Domenico, D. Wendisch, M. Grasshoff, T. S. Kapellos, M. Beckstette, T. Pecht, A. Saglam, O. Dietrich, H. E. Mei, A. R. Schulz, C. Conrad, D. Kunkel, E. Vafadarnejad, C.-J. Xu, A. Horne, M. Herbert, A. Drews, C. Thibeault, M. Pfeiffer, S. Hippenstiel, A. Hocke, H. Müller-Redetzky, K.-M. Heim, F. Machleidt, A. Uhrig, L. Bosquillon de Jarcy, L. Jürgens, M. Stegemann, C. R. Glösenkamp, H.-D. Volk, C. Goffinet, M. Landthaler, E. Wyler, P. Georg, M. Schneider, C. Dang-Heine, N. Neuwinger, K. Kappert, R. Tauber, V. Corman, J. Raabe, K. M. Kaiser, M. T. Vinh, G. Rieke, C. Meisel, T. Ulas, M. Becker, R. Geffers, M. Witzenrath, C. Drosten, N. Suttorp, C. von Kalle, F. Kurth, K. Händler, J. L. Schultze, A. C. Aschenbrenner, Y. Li, J. Nattermann, B. Sawitzki, A.-E. Saliba, L. E. Sander, A. Angelov, R. Bals, A. Bartholomäus, A. Becker, D. Bezdan, E. Bonifacio, P. Bork, T. Clavel, M. Colome-Tatche, A. Diefenbach, A. Dilthey, N. Fischer, K. Förstner, J.-S. Frick, J. Gagneur, A. Goesmann, T. Hain, M. Hummel, S. Janssen, J. Kalinowski, R. Kallies, B. Kehr, A. Keller, S. Kim-Hellmuth, C. Klein, O. Kohlbacher, J. O. Korbel, I. Kurth, M. Landthaler, Y. Li, K. Ludwig, O. Makarewicz, M. Marz, A. McHardy, C. Mertes, M. Nöthen, P. Nürnberg, U. Ohler, S. Ossowski, J. Overmann, S. Peter, K. Pfeffer, A. R. Poetsch, A. Pühler, N. Rajewsky, M. Ralser, O. Rieß, S. Ripke, U. Nunes da Rocha, P. Rosenstiel, A.-E. Saliba, L. E. Sander, B. Sawitzki, P. Schiffer, E.-C. Schulte, J. L. Schultze, A. Sczyrba, O. Stegle, J. Stoye, F. Theis, J. Vehreschild, J. Vogel, M. von Kleist, A. Walker, J. Walter, D. Wieczorek, J. Ziebuhr, Severe COVID-19 Is Marked by a Dysregulated Myeloid Cell Compartment, *Cell* **182**, 1419-1440.e23 (2020).

31. L. Wei, W. Wang, D. Chen, B. Xu, Dysregulation of the immune response affects the outcome of critical COVID-19 patients, *Journal of Medical Virology* **92**, 2768–2776 (2020).

32. R. L. Hoiland, N. A. Fergusson, A. R. Mitra, D. E. G. Griesdale, D. V. Devine, S. Stukas, J. Cooper, S. Thiara, D. Foster, L. Y. C. Chen, A. Y. Y. Lee, E. M. Conway, C. L. Wellington, M. S. Sekhon, The association of ABO blood group with indices of disease severity and multiorgan dysfunction in COVID-19, *Blood Advances* **4**, 4981–4989 (2020).

33. M. Hultström, B. Persson, O. Eriksson, M. Lipcsey, R. Frithiof, B. Nilsson, Blood type A associates with critical COVID-19 and death in a Swedish cohort, *Critical Care* **24**, 496 (2020).

34. M. B. Barnkob, A. Pottegård, H. Støvring, T. M. Haunstrup, K. Homburg, R. Larsen, M. B. Hansen, K. Titlestad, B. Aagaard, B. K. Møller, T. Barington, Reduced prevalence of SARS-CoV-2 infection in ABO blood group O, *Blood Advances* **4**, 4990–4993 (2020).

35. Y. Wu, Z. Feng, P. Li, Q. Yu, Relationship between ABO blood group distribution and clinical characteristics in patients with COVID-19, *Clinica Chimica Acta* **509**, 220–223 (2020).

36. S. Dzik, K. Eliason, E. B. Morris, R. M. Kaufman, C. M. North, COVID-19 and ABO blood groups, *Transfusion* **60**, 1883–1884 (2020).

37. J. M. O'Sullivan, S. Ward, H. Fogarty, J. S. O'Donnell, More on 'Association between ABO blood groups and risk of SARS-CoV-2 pneumonia,' *British Journal of Haematology* **190**, 27–28 (2020).

38. I. Huang, R. Pranata, Lymphopenia in severe coronavirus disease-2019 (COVID-19): systematic review and meta-analysis, *Journal of Intensive Care* **8**, 36 (2020).

39. C. I. van der Made, A. Simons, J. Schuurs-Hoeijmakers, G. van den Heuvel, T. Mantere, S. Kersten, R. C. van Deuren, M. Steehouwer, S. V. van Reijmersdal, M. Jaeger, T. Hofste, G. Astuti, J. Corominas Galbany, V. van der Schoot, H. van der Hoeven, W. Hagmolen of ten Have, E. Klijn, C. van den Meer, J. Fiddelaers, Q. de Mast, C. P. Bleeker-Rovers, L. A. B. Joosten, H. G. Yntema, C. Gilissen, M. Nelen, J. W. M. van der Meer, H. G. Brunner, M. G. Netea, F. L. van de Veerdonk, A. Hoischen, Presence of Genetic Variants Among Young Men With Severe COVID-19, *JAMA* **324**, 663–673 (2020).

40. Y. Li, M. Oosting, P. Deelen, I. Ricaño-Ponce, S. Smeekens, M. Jaeger, V. Matzaraki, M. A. Swertz, R. J. Xavier, L. Franke, C. Wijmenga, L. A. B. Joosten, V. Kumar, M. G. Netea, Inter-individual variability and genetic influences on cytokine responses to bacteria and fungi, *Nature Medicine* **22**, 952–960 (2016).

41. R. Aguirre-Gamboa, I. Joosten, P. C. M. Urbano, R. G. van der Molen, E. van Rijssen, B. van Cranenbroek, M. Oosting, S. Smeekens, M. Jaeger, M. Zorro, S. Withoff, A. E. van Herwaarden, F. C. G. J. Sweep, R. T. Netea, M. A. Swertz, L. Franke, R. J. Xavier, L. A. B. Joosten, M. G. Netea, C. Wijmenga, V. Kumar, Y. Li, H. J. P. M. Koenen, Differential Effects of Environmental and Genetic Factors on T and B Cell Immune Traits, *Cell Reports* **17**, 2474–2487 (2016).

42. M. Schirmer, S. P. Smeekens, H. Vlamakis, M. Jaeger, M. Oosting, E. A. Franzosa, R. ter Horst, T. Jansen, L. Jacobs, M. J. Bonder, A. Kurilshikov, J. Fu, L. A. B. Joosten, A.

Zhernakova, C. Huttenhower, C. Wijmenga, M. G. Netea, R. J. Xavier, Linking the Human Gut Microbiome to Inflammatory Cytokine Production Capacity, *Cell* **167**, 1125-1136.e8 (2016).

43. V. P. Mourits, V. A. C. M. Koeken, L. C. J. de Bree, S. J. C. F. M. Moorlag, W. C. Chu, X. Xu, H. Dijkstra, H. Lemmers, L. A. B. Joosten, Y. Wang, R. van Crevel, M. G. Netea, A. González, Ed. BCG-Induced Trained Immunity in Healthy Individuals: The Effect of Plasma Muramyl Dipeptide Concentrations, *Journal of Immunology Research* **2020**, 5812743 (2020).

44. T. S. Shah, J. Z. Liu, J. A. B. Floyd, J. A. Morris, N. Wirth, J. C. Barrett, C. A. Anderson, optiCall: a robust genotype-calling algorithm for rare, low-frequency and common variants, *Bioinformatics* **28**, 1598–1603 (2012).

45. P.-R. Loh, P. Danecek, P. F. Palamara, C. Fuchsberger, Y. A Reshef, H. K Finucane, S. Schoenherr, L. Forer, S. McCarthy, G. R. Abecasis, R. Durbin, A. L Price, Reference-based phasing using the Haplotype Reference Consortium panel, *Nature Genetics* **48**, 1443–1448 (2016).

46. X. Chu, M. Jaeger, O. B. Bakker, R. Aguirre-Gamboa, M. Oosting, S. P. Smeekens, S. Withoff, R. T. Netea-Maier, H. J. P. M. Koenen, I. Joosten, R. J. Xavier, L. Franke, L. a. B. Joosten, S. Sanna, V. Kumar, C. Wijmenga, M. G. Netea, Y. Li, in *European Journal of Human Genetics*, (Nature Publishing Group, 2019), vol. 27, pp. 787–787.

47. A. A. Shabalin, Matrix eQTL: ultra fast eQTL analysis via large matrix operations, *Bioinformatics.* **28** (2012), doi:10.1093/bioinformatics/bts163.

48. R. N. Tunjungputri, Y. Li, P. G. de Groot, C. A. Dinarello, S. P. Smeekens, M. Jaeger, M. Doppenberg-Oosting, M. Cruijsen, H. Lemmers, H. Toenhake-Dijkstra, R. Aguirre-Gamboa, V. Kumar, T. N. Wijmenga, L. A. B. Joosten, M. G. Netea, A. van der Ven, Q. de Mast, The inter-relationship of platelets with interleukin-1 β-mediated inflammation in humans, *Thrombosis and Haemostasis* **118**, 2112–2125 (2018).

49. C. Giambartolomei, D. Vukcevic, E. E. Schadt, L. Franke, A. D. Hingorani, C. Wallace, V. Plagnol, Bayesian Test for Colocalisation between Pairs of Genetic Association Studies Using Summary Statistics, *PLOS Genetics* **10**, e1004383 (2014).

A

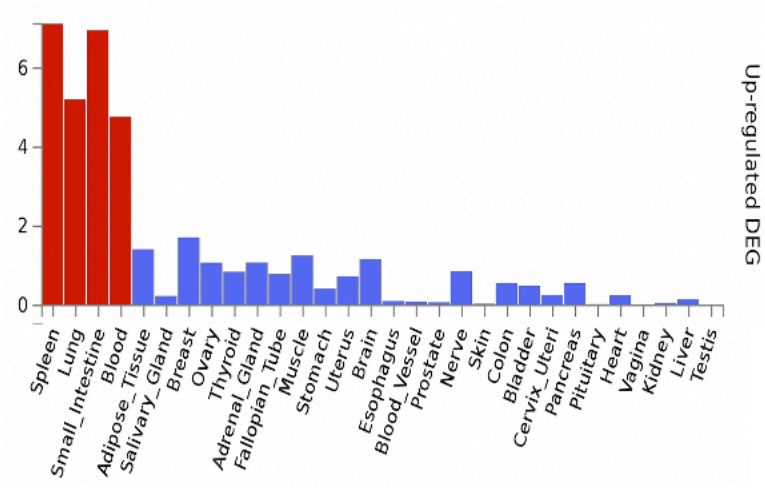

B

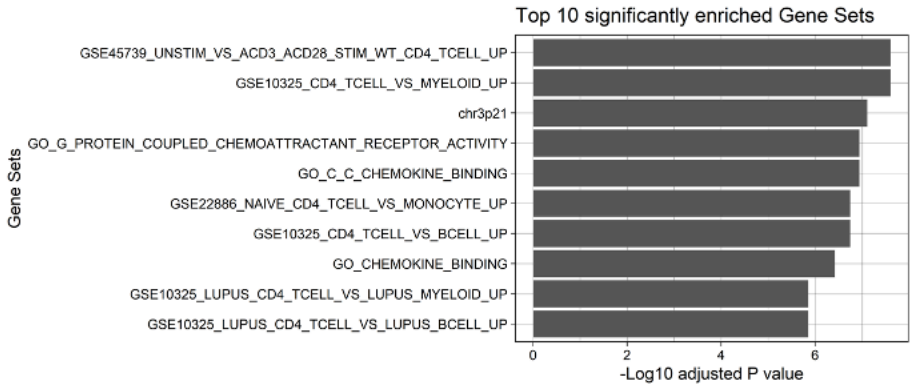

Fig.1. Functional annotation of COVID-19 loci using the FUMA pipeline. This was done based on genes identified after using FUMA to map QTLs based on their genomic location, eQTL associations, and histone activity. A) MAGMA Tissue expression results on 30 general tissues type (GTEx v8), B) The top 10 significant enriched gene sets.

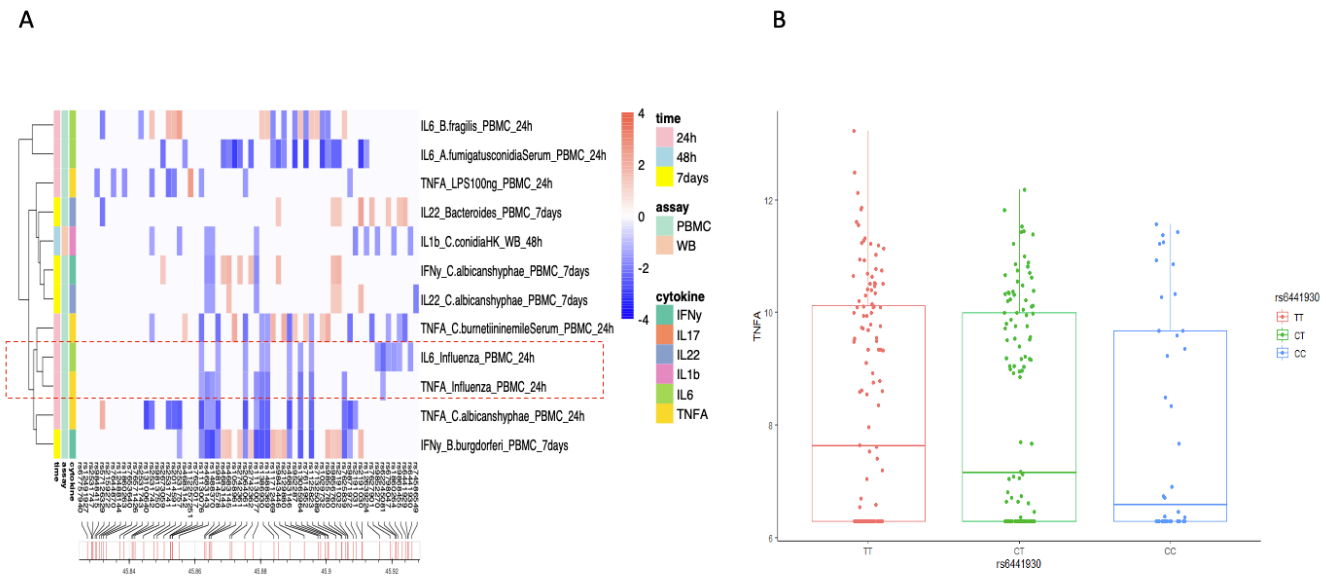

Fig. 2. The correlations between 3p21.31 loci and immune traits. Red bar in heatmap indicates higher cytokine production leaded by risk allele in COVID-19 GWAS profiles, Blue bar indicates lower cytokine production leaded by risk allele in COVID-19 GWAS profiles. A) the correlation between 3p21.31 with cytokine production upon *in vitro* stimulations B) a boxplot showing COVID-19 risk allele(rs6441930-C) associated with reduced IL6 production with influenza stimulation of PBMC for 24 hours (p-value = 0.026).

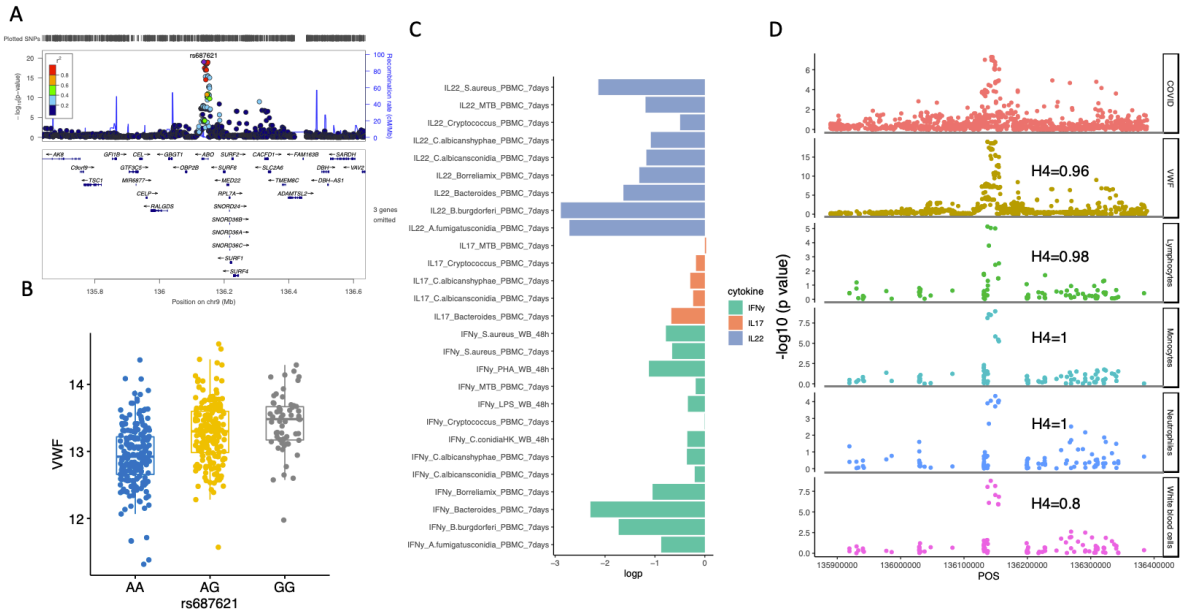

Fig 3. Functional annotation of ABO loci. A) locus zoom plot showing the significant association between ABO loci and VWF level. B) a boxplot showing COVID-19 risk allele(rs687621-G) associated with increasing VWF level (p-value = 9.58×10^{-20}). C) a barplot showing consistent negative correlations between VWF levels and T cell-derived cytokines D) scatter plots showing colocalization between ABO loci with VWF, lymphocytes, monocytes, neutrophils and white blood cell counts.

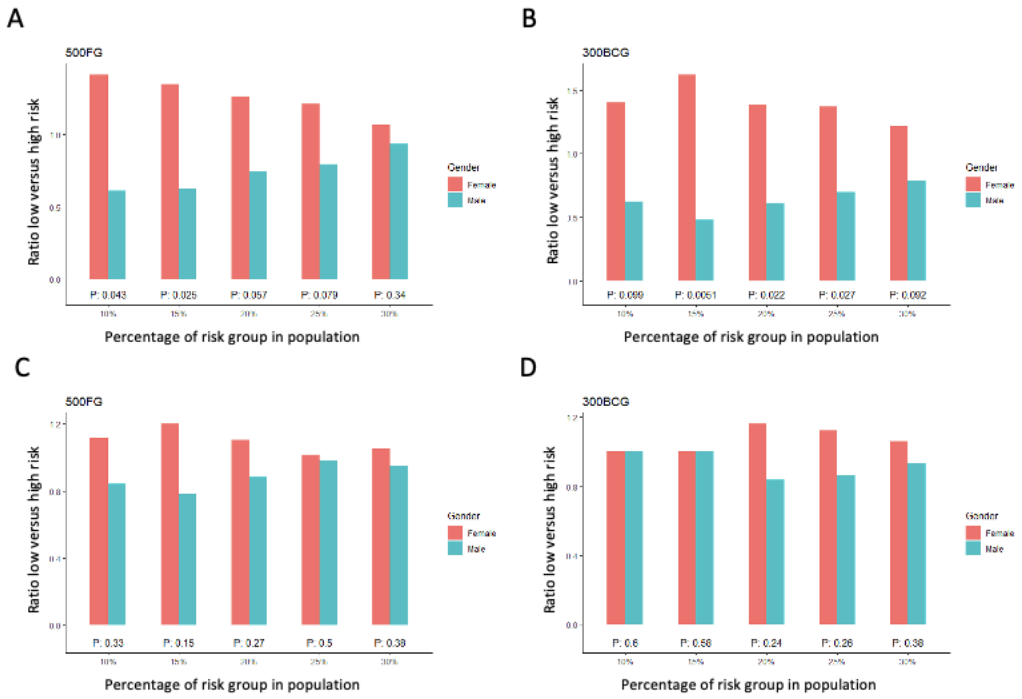

Fig. 4. Correlation of COVID-19 PRS with gender. A) bar plot representing the ratio of low risk versus high risk in 500FG. The X-axis shows the range of different quantiles (e.g.,10% corresponds to those individuals with PRS between 0th and 10th percentile of the population), and the Y-axis shows the odds ratio when comparing low PRS risk and high PRS risk in the male and female group from different quantiles. B) bar plot representing the ratio of low risk versus high risk in 300BCG. C) Bar plot representing the ratio of low versus high PRS based risk between men and women in 500FG calculated without including the sex chromosomes. D). Bar plot representing the ratio of low versus high PRS based risk between men and women in 300BCG calculated without including the sex chromosomes.

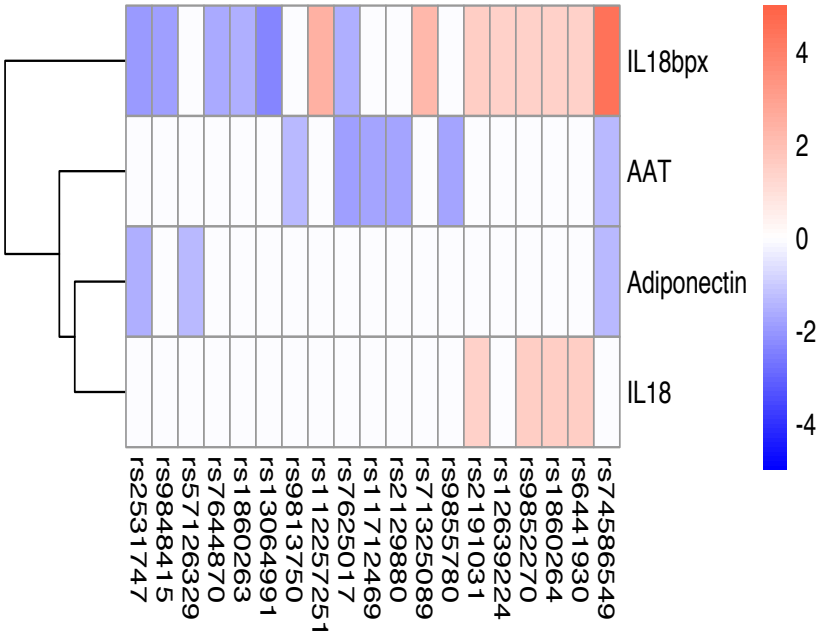

Fig. S1 Heatmap of the genetic correlations between 3p21.31 loci and circulating mediator.

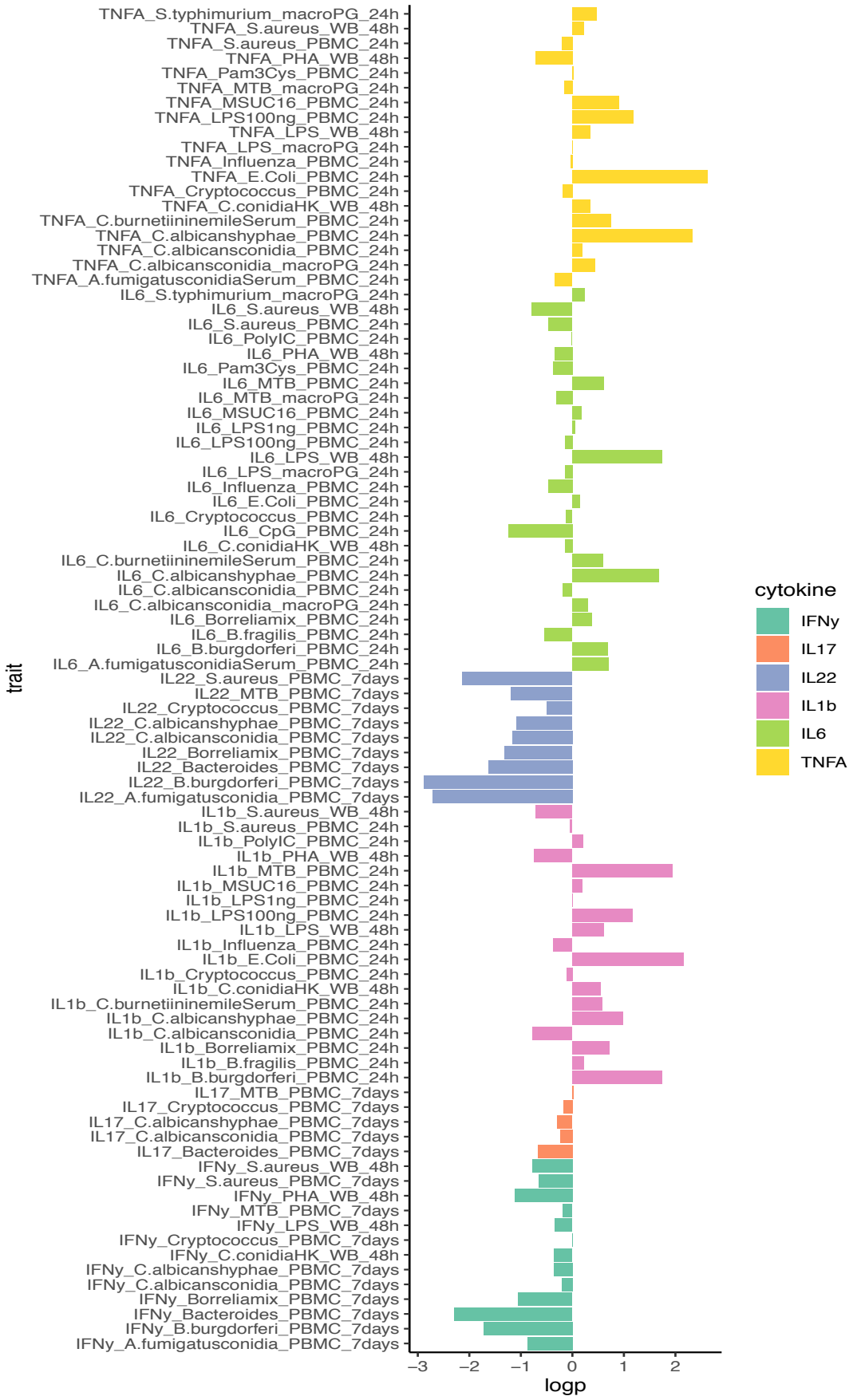

Fig. S2 A barplot showing correlations between VWF levels and cytokines.

A

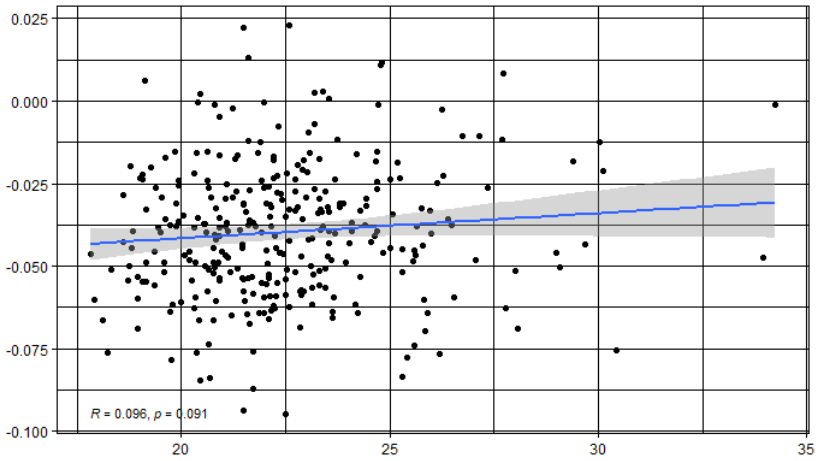

B

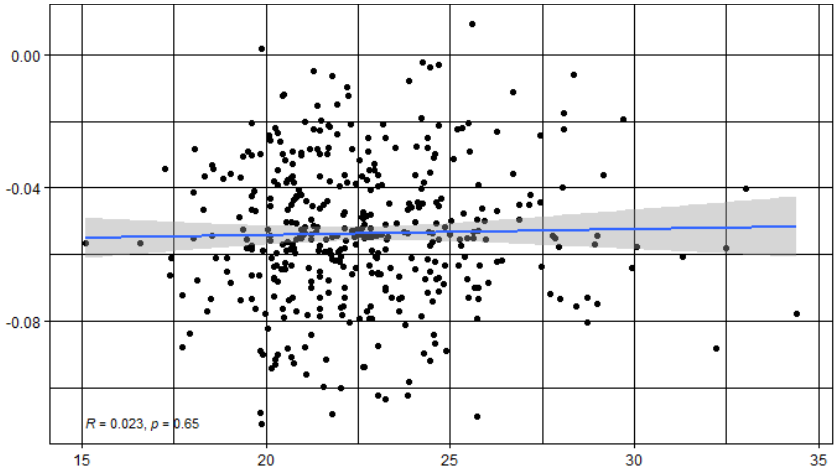

Fig. S3 Scatter plot showing the correlation between PRS with BMI A) in 500FG B) in 300BCG.

Table S1: Numbers and basic characteristics of participants included in the study.

	500FG (N = 451)	300BCG (N = 313)
Age (years)		
mean (SD)	28.1 (13.5)	25.9 (10.6)
median [Min, Max]	23 [18, 75]	23 [18, 71]
Sex		
Male sex: N (%)	211 (43.1%)	141 (43.3%)
BMI		
mean (SD)	22.8 (2.91)	22.5 (2.56)
median [Min, Max]	22.2 [15.1, 34.6]	22.1 [17.8, 34.2]
Smoking behaviour		
Smoker *: N (%)	85 (20.3%)	63 (20.2%)
Missing	32	0

SD = standard deviation
* Smokers were classified as people who regularly smoked or did so in the past.

Tabel S2 the assoication of COVID-19 risk loci with phenotypes in GWAS catalog (last accessed on 15-July-2020)

SNP	Mapped gene	Trait(s)	Study accession
rs505922-C	ABO	venous thromboembolism	GCST000354
rs505922-C	ABO	pancreatic carcinoma	GCST000456
rs8176719-G	ABO	malaria	GCST001637
rs505922-T	ABO	von Willebrand factor measurement	GCST001798

rs505922-?	ABO	tumor necrosis factor-alpha measurement	GCST000189
rs507666-G	ABO	ICAM-1 measurement	GCST000210
rs505922-?	ABO	Graves disease	GCST001982
rs8176719-G	ABO	venous thromboembolism	GCST001557
rs2519093-A	ABO	venous thromboembolism	GCST001557
rs507666-A	ABO	ICAM-1 measurement	GCST001047
rs505922-T	ABO	duodenal ulcer	GCST001433
rs505922-T	ABO	Graves disease	GCST001200
rs612169-G	ABO	metabolite measurement	GCST001217
rs505922-C	ABO	venous thromboembolism	GCST001253
rs8176685-G	ABO	platelet component distribution width	GCST004616
rs505922-C	ABO	type II diabetes mellitus	GCST005414
rs507666-?	ABO	e-selectin measurement	GCST004365
rs2519093-C	ABO	low density lipoprotein cholesterol measurement	GCST007141
rs2519093-C	ABO	low density lipoprotein cholesterol measurement	GCST007141
rs2519093-C	ABO	low density lipoprotein cholesterol measurement	GCST007141
rs2519093-C	ABO	low density lipoprotein cholesterol measurement	GCST007141
rs507666-G	ABO	low density lipoprotein cholesterol measurement	GCST007141
rs507666-G	ABO	low density lipoprotein cholesterol measurement	GCST007141
rs507666-G	ABO	low density lipoprotein cholesterol measurement	GCST007141
rs507666-A	ABO	low density lipoprotein cholesterol measurement	GCST002321

rs507666-A	ABO	total cholesterol measurement	GCST002321
rs505922-?	ABO	pancreatic carcinoma	GCST002991
rs505922-?	ABO	alkaline phosphatase measurement, clinical laboratory measurement	GCST003540
rs2519093-T	ABO	coronary artery disease	GCST003116
rs8176685-G	ABO	basophil count, eosinophil count	GCST004624
rs2519093-C	ABO	total cholesterol measurement	GCST007143
rs2519093-C	ABO	total cholesterol measurement	GCST007143
rs2519093-C	ABO	total cholesterol measurement	GCST007143
rs507666-G	ABO	total cholesterol measurement	GCST007143
rs507666-G	ABO	total cholesterol measurement	GCST007143
rs507666-G	ABO	total cholesterol measurement	GCST007143
rs115478735-T	ABO	blood protein measurement	GCST005806
rs115478735-T	ABO	blood protein measurement	GCST005806
rs2519093-?	ABO	alkaline phosphatase measurement	GCST006016
rs8176719-?	ABO	factor VIII measurement	GCST007445
rs8176719-?	ABO	factor VIII measurement	GCST007445
rs2519093-T	ABO	e-selectin measurement	GCST008202
rs2519093-T	ABO	ICAM-1 measurement	GCST008210
rs2519093-?	ABO	sleep duration, low density lipoprotein cholesterol measurement	GCST009365
rs2519093-T	ABO	venous thromboembolism	GCST009030
rs2519093-T	ABO	low density lipoprotein cholesterol measurement	GCST006612
rs507666-A	ABO	Eczema, allergic rhinitis	GCST009717
rs507666-?	ABO	blood protein measurement	GCST010104
rs507666-?	ABO	blood protein measurement	GCST010104
rs507666-?	ABO	blood protein measurement	GCST010104
rs507666-A	ABO	blood protein measurement	GCST008478

rs2519093-?	ABO	eosinophil count	GCST007065
rs2519093-?	ABO	leukocyte count	GCST007070
rs495828-A	AL772161.2, ABO	angiotensin converting enzyme activity measurement	GCST000565
rs495828-T	AL772161.2, ABO	erythrocyte count	GCST000588
rs495828-T	AL772161.2, ABO	hematocrit	GCST000583
rs495828-T	AL772161.2, ABO	alkaline phosphatase measurement	GCST000583
rs495828-T	AL772161.2, ABO	hemoglobin measurement	GCST000583
rs579459-C	ABO, AL772161.2	e-selectin measurement	GCST000476
rs579459-C	ABO, AL772161.2	coronary heart disease	GCST000998
rs579459-T	ABO, AL772161.2	adhesion molecule measurement, soluble P-selectin measurement	GCST000599
rs579459-T	ABO, AL772161.2	alkaline phosphatase measurement	GCST001276
rs495828-T	AL772161.2, ABO	venous thromboembolism	GCST001557
rs579459-C	ABO, AL772161.2	stroke, coronary heart disease	GCST002287
rs579459-C	ABO, AL772161.2	coronary heart disease	GCST002289
rs579459-?	ABO, AL772161.2	large artery stroke, coronary heart disease	GCST002290
rs579459-T	ABO, AL772161.2	urinary metabolite measurement	GCST002364
rs579459-T	ABO, AL772161.2	urinary metabolite measurement	GCST002364
rs579459-T	ABO, AL772161.2	total cholesterol measurement	GCST004231
rs579459-T	ABO, AL772161.2	low density lipoprotein cholesterol measurement	GCST004233
rs579459-T	ABO, AL772161.2	low density lipoprotein cholesterol measurement	GCST004233
rs579459-T	ABO, AL772161.2	low density lipoprotein cholesterol measurement	GCST007141
rs579459-T	ABO, AL772161.2	low density lipoprotein cholesterol measurement	GCST007141

rs579459-T	ABO, AL772161.2	low density lipoprotein cholesterol measurement	GCST007141
rs579459-T	ABO, AL772161.2	low density lipoprotein cholesterol measurement	GCST007141
rs495828-T	AL772161.2, ABO	blood metabolite measurement	GCST002442
rs579459-T	ABO, AL772161.2	blood metabolite measurement	GCST002442
rs579459-T	ABO, AL772161.2	erythrocyte count	GCST001765
rs633862-A	AL772161.2, ABO	Malignant epithelial tumor of ovary	GCST002576
rs579459-C	ABO, AL772161.2	total cholesterol measurement	GCST003214
rs579459-C	ABO, AL772161.2	low density lipoprotein cholesterol measurement	GCST003216
rs579459-C	ABO, AL772161.2	HbA1c measurement	GCST007954
rs579459-T	ABO, AL772161.2	total cholesterol measurement	GCST007143
rs579459-T	ABO, AL772161.2	total cholesterol measurement	GCST007143
rs579459-T	ABO, AL772161.2	total cholesterol measurement	GCST007143
rs495828-T	AL772161.2, ABO	triglyceride measurement, alcohol drinking	GCST008083
rs495828-T	AL772161.2, ABO	low density lipoprotein cholesterol measurement, alcohol drinking	GCST008079
rs495828-T	AL772161.2, ABO	triglyceride measurement, alcohol drinking	GCST008083
rs495828-T	AL772161.2, ABO	low density lipoprotein cholesterol measurement, alcohol drinking	GCST008079
rs495828-T	AL772161.2, ABO	low density lipoprotein cholesterol measurement, alcohol consumption measurement	GCST008078
rs495828-T	AL772161.2, ABO	triglyceride measurement, alcohol consumption measurement	GCST008074
rs600038-C	ABO, AL772161.2	heart failure	GCST009541

rs579459-C	ABO, AL772161.2	venous thromboembolism	GCST009030
rs579459-C	ABO, AL772161.2	blood protein measurement	GCST006585
rs579459-C	ABO, AL772161.2	blood protein measurement	GCST006585
rs579459-C	ABO, AL772161.2	blood protein measurement	GCST006585
rs579459-C	ABO, AL772161.2	blood protein measurement	GCST006585
rs579459-C	ABO, AL772161.2	blood protein measurement	GCST006585
rs579459-C	ABO, AL772161.2	blood protein measurement	GCST006585
rs579459-C	ABO, AL772161.2	blood protein measurement	GCST006585
rs579459-C	ABO, AL772161.2	blood protein measurement	GCST006585
rs579459-C	ABO, AL772161.2	blood protein measurement	GCST006585
rs579459-C	ABO, AL772161.2	blood protein measurement	GCST006585
rs579459-C	ABO, AL772161.2	blood protein measurement	GCST006585
rs579459-C	ABO, AL772161.2	blood protein measurement	GCST006585
rs579459-C	ABO, AL772161.2	blood protein measurement	GCST006585
rs579459-C	ABO, AL772161.2	blood protein measurement	GCST006585
rs579459-C	ABO, AL772161.2	blood protein measurement	GCST006585
rs579459-C	ABO, AL772161.2	blood protein measurement	GCST006585
rs579459-C	ABO, AL772161.2	blood protein measurement	GCST006585
rs579459-C	ABO, AL772161.2	blood protein measurement	GCST006585
rs579459-C	ABO, AL772161.2	blood protein measurement	GCST006585
rs579459-C	ABO, AL772161.2	blood protein measurement	GCST006585
rs579459-C	ABO, AL772161.2	blood protein measurement	GCST006585
rs579459-C	ABO, AL772161.2	blood protein measurement	GCST006585
rs579459-C	ABO, AL772161.2	blood protein measurement	GCST006585
rs579459-C	ABO, AL772161.2	blood protein measurement	GCST006585
rs579459-C	ABO, AL772161.2	blood protein measurement	GCST006585

rs579459-C	ABO, AL772161.2	blood protein measurement	GCST006585
rs579459-C	ABO, AL772161.2	blood protein measurement	GCST006585
rs579459-C	ABO, AL772161.2	blood protein measurement	GCST006585
rs579459-C	ABO, AL772161.2	blood protein measurement	GCST006585
rs579459-C	ABO, AL772161.2	blood protein measurement	GCST006585
rs579459-C	ABO, AL772161.2	blood protein measurement	GCST006585
rs579459-C	ABO, AL772161.2	blood protein measurement	GCST006585
rs495828-T	AL772161.2, ABO	blood protein measurement	GCST008478
rs495828-?	AL772161.2, ABO	Eczema	GCST007075
rs507666-A	ABO	total cholesterol measurement	GCST002896
rs2519093-?	ABO	allergy	GCST003990
rs507666-G	ABO	pulse pressure measurement	GCST007096
rs507666-G	ABO	diastolic blood pressure	GCST007094
rs8176643-A	ABO	hemoglobin measurement	GCST004615
rs8176643-?	ABO	susceptibility to childhood ear infection measurement	GCST005013
rs505922-C	ABO	CD209 antigen measurement	GCST004365
rs505922-C	ABO	Ischemic stroke, von Willebrand factor measurement, homocysteine measurement	GCST004598
rs2519093-T	ABO	venous thromboembolism	GCST004256
rs8176645-A	ABO	venous thromboembolism	GCST004256
rs8176643-A	ABO	hematocrit	GCST004604
rs612169-G	ABO	von Willebrand factor measurement	GCST004365
rs507666-A	ABO	coronary artery disease	GCST004787
rs2519093-T	ABO	blood protein measurement	GCST005806
rs2519093-T	ABO	blood protein measurement	GCST005806
rs2519093-T	ABO	blood protein measurement	GCST005806
rs2519093-T	ABO	blood protein measurement	GCST005806

rs2519093-T	ABO	blood protein measurement	GCST005806
rs2519093-T	ABO	blood protein measurement	GCST005806
rs2519093-T	ABO	blood protein measurement	GCST005806
rs2519093-T	ABO	blood protein measurement	GCST005806
rs2519093-T	ABO	blood protein measurement	GCST005806
rs2519093-T	ABO	blood protein measurement	GCST005806
rs505922-C	ABO	pancreatic carcinoma	GCST005434
rs2519093-T	ABO	coronary artery disease	GCST005195
rs2519093-?	ABO	hematocrit	GCST005994
rs2519093-?	ABO	hemoglobin measurement	GCST005995
rs2519093-?	ABO	erythrocyte count	GCST005996
rs507666-A	ABO	coronary artery disease	GCST005196
rs505922-C	ABO	peripheral arterial disease	GCST008474
rs8176685-?	ABO	von Willebrand factor measurement	GCST007446
rs8176719-?	ABO	von Willebrand factor measurement	GCST007446
rs8176643-A	ABO	blood protein measurement	GCST005806
rs8176643-A	ABO	blood protein measurement	GCST005806
rs8176643-A	ABO	blood protein measurement	GCST005806
rs8176643-A	ABO	blood protein measurement	GCST005806
rs8176685-?	ABO	von Willebrand factor measurement	GCST007446
rs505922-C	ABO	type II diabetes mellitus	GCST009379
rs2519093-?	ABO	sleep duration, low density lipoprotein cholesterol measurement	GCST009366
rs507666-A	ABO	e-selectin measurement	GCST009572
rs507666-A	ABO	low density lipoprotein cholesterol measurement, physical activity	GCST007284
rs2519093-T	ABO	allergic rhinitis	GCST006409
rs505922-C	ABO	blood protein measurement	GCST005806
rs505922-C	ABO	blood protein measurement	GCST005806

rs507666-A	ABO	blood protein measurement	GCST005806
rs507666-A	ABO	blood protein measurement	GCST005806
rs2519093-T	ABO	HMG CoA reductase inhibitor use measurement	GCST007931
rs507666-?	ABO	total cholesterol measurement	GCST008045
rs2769071-A	ABO	fibroblast growth factor 23 measurement	GCST006491
rs507666-?	ABO	low density lipoprotein cholesterol measurement	GCST008037
rs505922-C	ABO	disposition index measurement	GCST008111
rs495828-?	AL772161.2, ABO	erythrocyte count	GCST004008
rs495828-T	AL772161.2, ABO	hematocrit	GCST004003
rs579459-T	ABO, AL772161.2	erythrocyte count	GCST004008
rs495828-T	AL772161.2, ABO	hemoglobin measurement	GCST004005
rs495828-?	AL772161.2, ABO	hemoglobin measurement	GCST004005
rs579459-T	ABO, AL772161.2	low density lipoprotein cholesterol measurement	GCST004236
rs579459-T	ABO, AL772161.2	total cholesterol measurement	GCST004235
rs579459-T	ABO, AL772161.2	total cholesterol measurement	GCST004235
rs495828-T	AL772161.2, ABO	coronary artery disease	GCST005194
rs495828-T	AL772161.2, ABO	low density lipoprotein cholesterol measurement, alcohol drinking	GCST008086
rs495828-T	AL772161.2, ABO	low density lipoprotein cholesterol measurement, alcohol drinking	GCST008086
rs579459-?	ABO, AL772161.2	platelet reactivity measurement	GCST008457
rs495828-T	AL772161.2, ABO	low density lipoprotein cholesterol measurement, alcohol drinking	GCST008086
rs495828-T	AL772161.2, ABO	low density lipoprotein cholesterol measurement, alcohol drinking	GCST008086

rs495828-T	AL772161.2, ABO	low density lipoprotein cholesterol measurement, alcohol consumption measurement	GCST008078
rs495828-T	AL772161.2, ABO	low density lipoprotein cholesterol measurement, alcohol consumption measurement	GCST008078
rs495828-T	AL772161.2, ABO	low density lipoprotein cholesterol measurement, alcohol consumption measurement	GCST008078
rs495828-T	AL772161.2, ABO	low density lipoprotein cholesterol measurement	GCST008077
rs495828-T	AL772161.2, ABO	low density lipoprotein cholesterol measurement	GCST008077
rs495828-T	AL772161.2, ABO	low density lipoprotein cholesterol measurement, alcohol drinking	GCST008079
rs495828-T	AL772161.2, ABO	low density lipoprotein cholesterol measurement, alcohol drinking	GCST008079
rs495828-T	AL772161.2, ABO	low density lipoprotein cholesterol measurement	GCST008077
rs579459-T	ABO, AL772161.2	low density lipoprotein cholesterol measurement	GCST008676
rs495828-T	AL772161.2, ABO	tissue factor measurement	GCST009731
rs495828-T	AL772161.2, ABO	hemoglobin measurement	GCST010083
rs579459-C	ABO, AL772161.2	alkaline phosphatase measurement	GCST010047
rs579459-T	ABO, AL772161.2	blood protein measurement	GCST006585
rs579459-?	ABO, AL772161.2	total cholesterol measurement	GCST008045
rs579459-?	ABO, AL772161.2	low density lipoprotein cholesterol measurement	GCST008037
rs17764831-?	LZTFL1	eosinophil count	GCST007065

Table S3: Independent lead GWAS loci reported in NEJM (hg38) and in hg19*.

uniqID	rsID	p	nIndSigSNPs	IndSigSNPs
1:88993151:C:T	rs75558547	4.49E-06	1	rs75558547
2:15724310:A:G	rs2080811	1.12E-06	1	rs2080811
3:45876459:G:GA	rs11385942	1.15E-10	3	rs11385942;rs34901975;rs3774641
3:149805983:C:G	rs144582715	7.17E-06	1	rs144582715
4:180344873:A:G	rs1455662	9.60E-06	1	rs1455662
6:20314719:C:T	rs911360	4.09E-06	1	rs911360
6:23379360:A:AT	rs5874914	4.64E-06	1	rs5874914
6:91010824:A:ATTAC	rs3073485	5.72E-06	1	rs3073485
7:123006727:A:G	rs12706520	9.63E-06	1	rs12706520
7:158020147:A:G	rs6970487	4.89E-06	1	rs6970487
8:122848829:A:G	rs10091098	4.55E-06	1	rs10091098
8:126952467:A:T	rs28730361	8.11E-06	1	rs28730361
9:136139265:A:C	rs657152	4.95E-08	3	rs657152;rs550057;rs647800
11:5691474:C:G	rs12796811	3.62E-06	1	rs12796811
12:62463979:G:T	rs10877786	6.89E-07	1	rs10877786
14:32422746:C:G	rs7152677	1.52E-06	1	rs7152677
16:74936031:A:G	rs2059266	4.01E-06	1	rs2059266
16:82338406:C:T	rs114093749	3.86E-06	2	rs114093749;rs4569267
17:10376558:G:T	rs117438562	7.49E-06	1	rs117438562
18:3724602:A:G	rs13381043	1.13E-07	2	rs13381043;rs4797120
18:22624707:A:G	rs56132597	8.94E-06	1	rs56132597
19:4717672:A:G	rs12610495	5.20E-06	1	rs12610495
19:5518492:C:T	rs183544391	7.29E-06	1	rs183544391
19:17923554:T:TC	rs3833287	4.24E-06	1	rs3833287
23:15138357:C:T	rs55634010	9.75E-06	1	rs55634010

23:146325425:A:T	rs10126492	8.81E-06	1	rs10126492

Table S4 Functional annotation of SNPs on genes by ANNOVAR*

annotation	ref.count	ref.prop	count	prop	enrichment	fisher.P
UTR3	233824	0.0093225	13	0.016	1.694	0.066
UTR5	71546	0.00285252	3	0.004	1.278	0.512
downstream	284177	0.01133006	8	0.010	0.858	0.868
exonic	254736	0.01015625	8	0.010	0.957	1.000
intergenic	11684523	0.46585868	378	0.459	0.986	0.727
intronic	9137749	0.36431951	329	0.400	1.097	0.036
ncRNA_exonic	259951	0.01036417	2	0.002	0.234	0.015
ncRNA_intronic	2884355	0.11499843	79	0.096	0.835	0.090
ncRNA_splicing	1313	5.23E-05	0	0.000	0.000	1.000
splicing	2830	0.00011283	0	0.000	0.000	1.000
upstream	266686	0.0106327	3	0.004	0.343	0.058

Table S5 Roadmap epigenetic state enrichment analysis

Regulatory* elements	total Bins	1.00E-05	1.00E-06	1.00E-07	P. 1E-5	P. 1E-6	P. 1E-7
Active enhancer states	2068209	129	34	10	2.96E-25	6.76E-12	0.042
Active promotor states	513015	31	15	0	4.86E-06	1.59E-08	0.63
All enhancer states	2133264	133	37	10	7.26E-26	1.35E-13	0.042
All promotor states	525189	31	15	0	8.36E-06	1.62E-08	0.63
Whole Genome	15282831	368	71	34			

*Enhancer and promoter states were derived from a 15-state model based on five chromatin marks; the core set of five histone modification marks was shared by 127 reference epigenomes of 24 blood cells from the Roadmap Epigenomics project. Promoter states include active promoter states (TssA , TssAFlnk) and inactive states (TssBiv); Enhancer states include active enhancer states (Enh, EnhG) and inactive states (EnhBiv). Enrichment of COVID-19 loci in regulatory elements was estimated by using Fisher's exact test.

Table S6 Comparsion polygeneic risk score(PRS) between male and female in 500FG (N=451) and 300BCG (N=313).

Table continued (part 1)

Fraction	Risk group	Male -500FG	Female -500FG	OR (95% CI)	Pvalue-500FG*
10%	high risk	26	19	1.496 (0.980 - 2.283)	0.045
10%	low risk	17	28		
15%	high risk	32	35	1.235 (0.883 - 1.727)	0.147
15%	low risk	25	42		
20%	high risk	41	49	1.171 (0.876 - 1.566)	0.182
20%	low risk	34	56		
25%	high risk	53	59	1.176 (0.907 - 1.526)	0.140
25%	low risk	44	68		
30%	high risk	61	73	1.154 (0.909 - 1.465)	0.149
30%	low risk	52	83		

Table continued (part 2)

Male -300BCG	Female -300BCG	OR (95% CI)	Pvalue-300FG*	Meta-Pvalue**
15	17	1.434 (0.894 - 2.300)	0.115	0.011
9	22			
25	21	1.770 (1.182 - 2.650)	0.005	0.004
12	34			
33	29	1.524 (1.075 - 2.163)	0.014	0.010
20	42			
41	37	1.397 (1.022 - 1.910)	0.026	0.011
28	50			
45	48	1.163 (0.874 - 1.549)	0.188	0.051

38	55			

* the p value is obtained using the fisher extact test

** the p value is obtained using the meta analyzed z score approach

Table S7 Comparsion polygeneic risk score(PRS) between male and female in 500FG (N=451) and 300BCG (N=313) (age and gender corrected model)

Table continued (part 1)

Fraction	Risk group	Male -500FG	Female -500FG	OR (95% CI)	Pvalue-500FG*
10%	high risk	23	22	1.498 (0.997 - 2.249)	0.043
10%	low risk	14	31		
15%	high risk	32	35	1.442 (1.036 - 2.006)	0.025
15%	low risk	20	47		
20%	high risk	43	46	1.296 (0.969 - 1.734)	0.057
20%	low risk	32	58		
25%	high risk	53	58	1.231 (0.948 - 1.599)	0.079
25%	low risk	42	70		
30%	high risk	58	76	1.070 (0.841 - 1.361)	0.336
30%	low risk	54	81		

Table continued (part 2)

Male -300BCG	Female -300BCG	OR (95% CI)	Pvalue-300FG*	Meta-Pvalue**
16	15	1.477 (0.903 - 2.415)	0.099	0.030
10	21			
25	21	1.770 (1.182 - 2.650)	0.005	0.005
12	34			

31	31	1.48 (1.048 - 2.090)	0.022	0.008
19	43			
43	35	1.397 (1.018 - 1.917)	0.027	0.039
30	48			
47	46	1.241 (0.932 - 1.652)	0.092	0.214
37	56			

* the p value is obtained using the fisher extact test
** the p value is obtained using the meta analyzed z score approach

Table S8 The replication of ABO loci in COVID-19 Host genetics initiative(HGI) data

RSid	Effect Allele	Other Allele	Beta	SE	P^	P-HGI*
rs8176719	T	TC	-0.2772	0.052	9.93E-08	8.88E-07
rs633862	T	C	0.2534	0.0515	8.79E-07	2.80E-06

^Pvalue from D. Ellinghaus et.al New England Journal of Medicine 2020, DOI: 10.1056/NEJMoa2020283

*Pvalue from COVID-19 HGI (https://www.covid19hg.org/results/, last accessed 21st of October 2020). The effect allele has been aligned.